Entropy **2013**, *15*, 4782-4801; doi:10.3390/e15114782

OPEN ACCESS

entropy

ISSN 1099-4300

www.mdpi.com/journal/entropy

Article

Stochasticity: A Feature for the Structuring of Large and Heterogeneous Image Databases

Abdourrahmane M. Atto [1,*], Yannick Berthoumieu [2] and Rémi Mégret [2]

[1] LISTIC (Laboratory of Informatics, Systems, Information and Knowledge Processing), University of Savoie, B.P. 80439, 74944 Annecy le Vieux Cedex, France

[2] IMS (Laboratory of Material to System Integration), CNRS UMR 5218, University of Bordeaux, IPB, ENSEIRB-MATMECA, 351 cours de la libération, 33400 Talence, France

* Author to whom correspondence should be addressed; E-Mail: abdourrahmane.atto@univ-savoie.fr; Tel.: +33-450-096-527; Fax: +33-450-096-559.

Received: 26 August 2013; in revised form: 27 September 2013 / Accepted: 29 October 2013 / Published: 4 November 2013

Abstract: The paper addresses image feature characterization and the structuring of large and heterogeneous image databases through the stochasticity or randomness appearance. Measuring stochasticity involves finding suitable representations that can significantly reduce statistical dependencies of any order. Wavelet packet representations provide such a framework for a large class of stochastic processes through an appropriate dictionary of parametric models. From this dictionary and the Kolmogorov stochasticity index, the paper proposes semantic stochasticity templates upon wavelet packet sub-bands in order to provide high level classification and content-based image retrieval. The approach is shown to be relevant for texture images.

Keywords: texture descriptors; stochasticity measurements; semantic gap; parametric modeling

---

1. Introduction

The diversity of real world images has led researchers to take advantage of various mathematical tools in order to extract relevant image features or retrieve suitable information in images. For instance, probabilistic models, geometry properties and functional analysis have raised much dissertation in the last few decades. In practice, the selection of appropriate features is driven by the class of images of

interest. In this paper, the class of images we deal with can be conceptually defined through its departure from the class of regular images.

From the literature, a *regular* image is defined as either *smooth* or *geometrically regular* [1]: the image is composed of different smooth regions delimited by singularity curves. In contrast, a *non-regular* image is such that: when splitting the image into smaller and smaller subimages (sub-surfaces), almost every subimage is non-regular in that it is expected to contain many delimitation curves.

From the above consideration, a texture can be identified as either geometrically regular, *i.e.*, composed of different or repetitive regions that are smooth, except along their delimitation curves, or non-regular. Geometrically regular textures can be well characterized by local or global regularity measurements, such as Holder exponents [1–7] or spectral measurements [8–14]. In contrast, regularity measurements fail to be efficient for the characterization of non-regular textures, since measuring very low regularity parameters is not straightforward.

The approach proposed below to characterize non-regular textures involves the most relevant features that have proven useful in texture analysis [2,12,13]. These features are considered jointly in the framework of (1) *stochasticity*, a concept that relies on, but is not limited to, coarseness and roughness, and (2) wavelet packet transform, a representation that provides time-frequency, directionality, as well as other suitable statistical properties mentioned below.

The stochasticity degree (or randomness appearance) is hereafter measured by using the Kolmogorov stochasticity parameter [15]. This parameter is applied under the assumption that data are *independent and identically distributed* (iid), and their cumulative distribution function is completely specified. Recent works related to this parameter concern measuring the randomness degree of discrete sequences from dynamical systems and number theory [16], as well as measuring the contribution of randomness in the cosmic microwave background [17]. In these works, the Kolmogorov parameter has been used for specific datasets that are expected to comply with the underlying iid assumption, with a known distribution function.

In a more general framework involving real world textures, this iid assumption is very restrictive, due to non-stationarity, correlation and other more intricate statistical dependencies that occur among real world images.

The contributions of the present paper with respect to [16,17] concern relaxing these restrictive assumptions by:

(1) Considering the wavelet packet transform, a transform that makes it possible to distribute many random processes as stationary, independent and identically distributed sequences (see, for instance, [18–20]);

(2) Considering a dictionary of parametric models that are relevant with respect to the statistical distribution of the wavelet packet coefficients.

Under the above considerations, stochasticity can be measured even for correlated and non-stationary data through their wavelet packet representations. Furthermore, from the order structure that characterizes wavelet packet bases, we derive two different semantic templates for supporting a high level texture description: (1) generating a semantic stochasticity template upon a fixed wavelet packet basis; and (2) learning a wavelet packet tree structure that supports the best stochastic bases of training samples, provided that a critical stochasticity value is fixed.

The presentation of this paper is as follows. Section 2 introduces the Kolmogorov stochasticity parameter and assesses its relevance in detecting deterministic regular patterns. Section 3 addresses texture classification by using stochasticity templates. Section 4 presents the application of stochasticity analysis to standard content-based image retrieval by providing the stochastic structuring of databases. Section 5 provides semantic-based texture retrieval concepts and experimental results. Finally, Section 6 provides a conclusion to the paper.

2. Stochasticity Measurements

2.1. Kolmogorov Stochasticity Index: Deterministic Pattern

Let $x = (x_1, x_2, \ldots, x_N)$ be a sample set that follows from iid random variables with *probability density function* (pdf), f, and *cumulative distribution function* (cdf) F. The Kolmogorov stochasticity parameter [15] is:

$$\kappa(x, F) = \sup_t |F_{x,N}(t) - F(t)| \tag{1}$$

where $F_{x,N}$ is the empirical cdf of the N-sample sequence, x.

Standard approaches for testing random generators are based on binary hypothesis testing (stochastic or not) and focus on the asymptotic properties of $\sqrt{N}\kappa(x, F)$ when N tends to infinity. In contrast with these approaches, we assume no binary hypothesis, since we will use the heights of $\kappa(x, F)$ to compare textures in terms of their randomness appearances, whatever the values of the stochasticity indices.

Note that $\kappa(x, F) \ll 1$ for datasets that are stochastic with respect to F (a consequence of the Glivenko-Cantelli theorem). This implies that any x satisfying $\kappa(x, F) = 1$ is non-stochastic with respect to F. For instance, since we are dealing with a dictionary of continuous cdfs, we will say that a constant sequence is deterministic with respect to this dictionary: for such a sequence, the reader can check that $\sup |F_{x,N}(t) - F(t)| = 1$, as far as $N \geqslant 2$. Furthermore, we have that the presence of a value with large occurrence in a dataset can be qualified as a deterministic pattern, since it impacts, as well, $\sup |F_{x,N}(t) - F(t)|$.

The following section addresses the relevance of $\kappa(x, F)$ in pointing out deterministic patterns, in comparison with other stochasticity measures available in the literature.

2.2. The Relevance of the Kolmogorov Stochasticity Parameter in Detecting Deviations From a Specified Distribution

The results presented in this section concern the sensitivity of different stochasticity measures when data with a given stochasticity degree are corrupted with elementary deterministic patterns with increasing sizes.

There are basically two criteria that distinguish stochasticity measures:

(1) The norm used, which can be cumulative or uniform;

(2) The distribution, which can be specified as pdf or cdf.

Some examples issued from random generator testing are a) the Kolmogorov-Smirnov test [21], based on the uniform (ℓ_∞) norm and comparing two cdfs in a binary hypothesis testing, b) the chi-squared test [22], based on the cumulative ℓ_2 norm and comparing two pdfs in a binary hypothesis testing problem.

Let us consider an N-size dataset (texture image for instance) with a stochasticity degree, η, with respect to a given distribution model. Assume that these data are affected by a deterministic pattern in the sense that a proportion, K/N, of the data is set to a constant value, where K is the size of the pattern under consideration. Since a stochasticity measure can be seen as a dissimilarity measure between distribution functions, a relevant stochasticity measure is such that its stochasticity parameter should increases as K increases (the randomness appearance of the texture has decreased).

In the following experiments, a deterministic pattern consisting of the insertion of K occurrences of a fixed value is introduced into datasets, and the relevance of different stochasticity measures is tested when the size K of this pattern increases. These experiments are performed upon the detail wavelet coefficients of textured images. These coefficients are expected to be very small in smooth regions and large in the neighborhood of edges. Increasing the number of null coefficients, if any, by forcing K large coefficients to zero (deterministic pattern) results in smoothing some edges of the image. This implies reducing the intrinsic stochasticity of the data when K increases. A relevant stochasticity measure should depart from the initial stochasticity degree when K increases.

Table 1. Experimental setup for testing the relevance of the uniform (ℓ_∞) norm *versus* the cumulative ℓ_2 norm and Kullback-Leibler divergence (KLD) in stochasticity measurements. The quantities involved in the computation of the relative stochasticity value (RSV) are the empirical distribution and the model. cdf: cumulative distribution function.

For $0 \leqslant K \leqslant 150$, **do:**

Compute the wavelet coefficients, $(c_{j,n})_{j,n}$, of the input image.

Introduce a deterministic pattern among the coefficients of a sub-band by setting the K largest coefficients to zero (notation: $\left(c^K_{j,n}\right)_{j,n}$).

Compute the stochasticity parameters:

Check the distribution type from the variable "specification"

Case specification is "cdf", **then**:

$$\text{Compute RSV}(K) = \frac{\left\| F_{c^K_{j,n},N} - F_\theta\left(c^K_{j,n}\right) \right\|}{\left\| F_{c^0_{j,n},N} - F_\theta\left(c^0_{j,n}\right) \right\|}$$

Case specification is "pdf", **then**:

$$\text{Compute RSV}(K) = \frac{\left\| f_{c^K_{j,n},N} - f_\theta\left(c^K_{j,n}\right) \right\|}{\left\| f_{c^0_{j,n},N} - f_\theta\left(c^0_{j,n}\right) \right\|}$$

End

Compare the measurements obtained: for a relevant stochasticity measure, RSV is a non-decreasing function of K.

We consider the experimental setup presented in Table 1: different combinations between norms (ℓ_2, ℓ_∞) and distribution specifications (cdf, pdf) are used for testing stochasticity measures. In this table, $||\cdot||$ specifically denotes either the ℓ_∞ and ℓ_2 norms. The Kullback-Leibler Divergence (KLD) is also used for comparison purposes. The Kullback-Leibler similarity measure between random variables, X_1 and X_2, having probability distribution functions f_{X_1} and f_{X_2} is defined as:

$$\mathcal{K}(X_1, X_2) = \mathcal{K}(X_1||X_2) + \mathcal{K}(X_2||X_1) \tag{2}$$

$$\text{with} \qquad \mathcal{K}(X_i||X_j) = \int_{\mathbb{R}} f_{X_i}(x) \log \frac{f_{X_i}(x)}{f_{X_j}(x)} dx, \quad i, j = 1, 2.$$

In addition, if $c_{j,n}$ denotes the wavelet packet coefficients obtained at sub-band $\mathbf{W}_{j,n}$, then $c_{j,n}^K$ corresponds to the dataset obtained by setting the K largest values of $c_{j,n}$ to zero. In particular, $c_{j,n}^0 = c_{j,n}$.

Figure 1. Relative stochasticity values for the image "Fabric.0004" from the VisTeX database. The RSV of a relevant stochasticity measurement must be an increasing function of the size K of the deterministic pattern. We have $K = 0, 10, 20, \ldots, 150$ and $N = 68,644$. (**a**) cdf-based stochasticity measures; (**b**) pdf-based stochasticity measures.

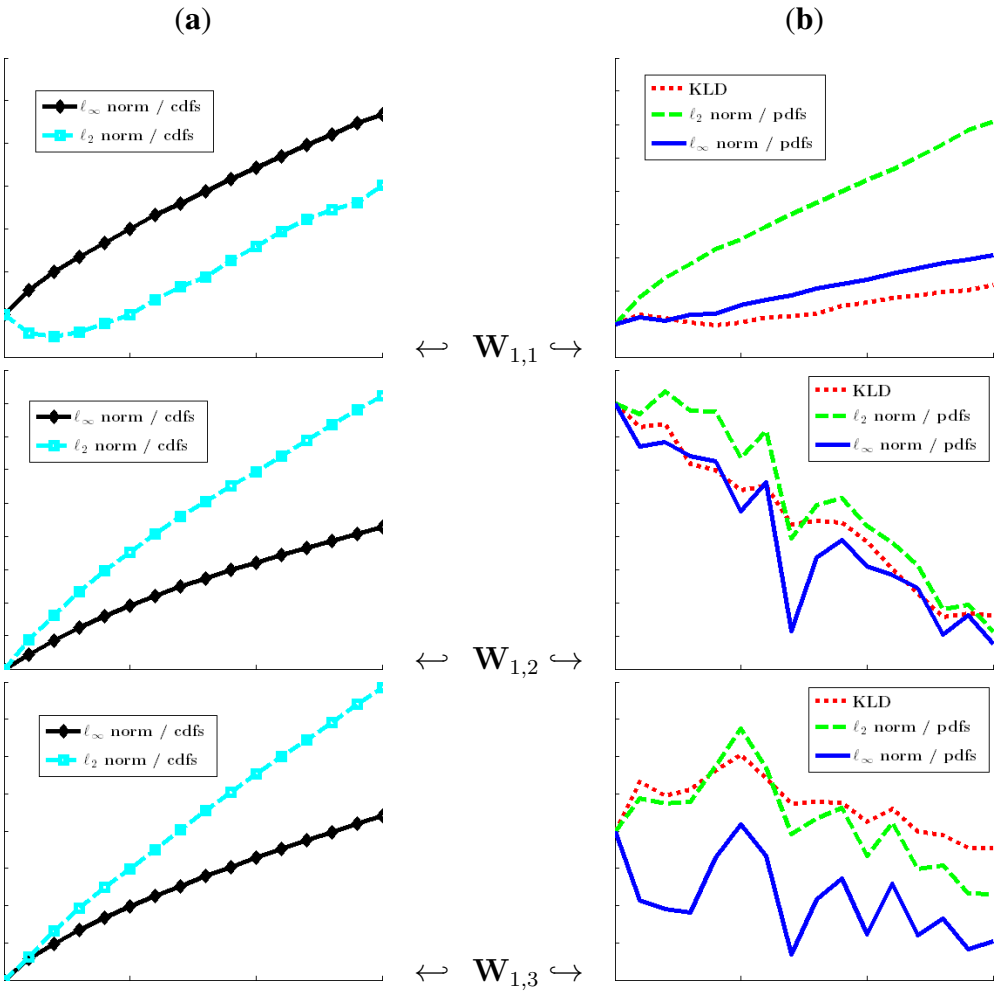

Departure from the initial stochasticity value of the wavelet coefficients is measured with respect to the *generalized Gaussian* distributions. In addition, Gaussian, triangle and Epanechnikov kernels

have been used for the estimation of the empirical pdfs involved in Table 1. The results provided in Figures 1 and 2 are obtained with a Gaussian kernel, and the wavelet decomposition has been performed with a Daubechies wavelet function of order seven. These results concern the images "Fabric.0004" and "Fabric.0018" from the VisTeX database (see Figure 1). Results are similar for other textures from the VisTeX database and for other kernels (concerning pdf-based measures).

Figure 2. Relative stochasticity values for the image "Fabric.0018" from the VisTeX database. The RSV of a relevant stochasticity measurement must be an increasing function of the size K of the deterministic pattern. We have $K = 0, 10, 20, \ldots, 150$ and $N = 68,644$. (**a**) cdf-based stochasticity measures; (**b**) pdf-based stochasticity measures.

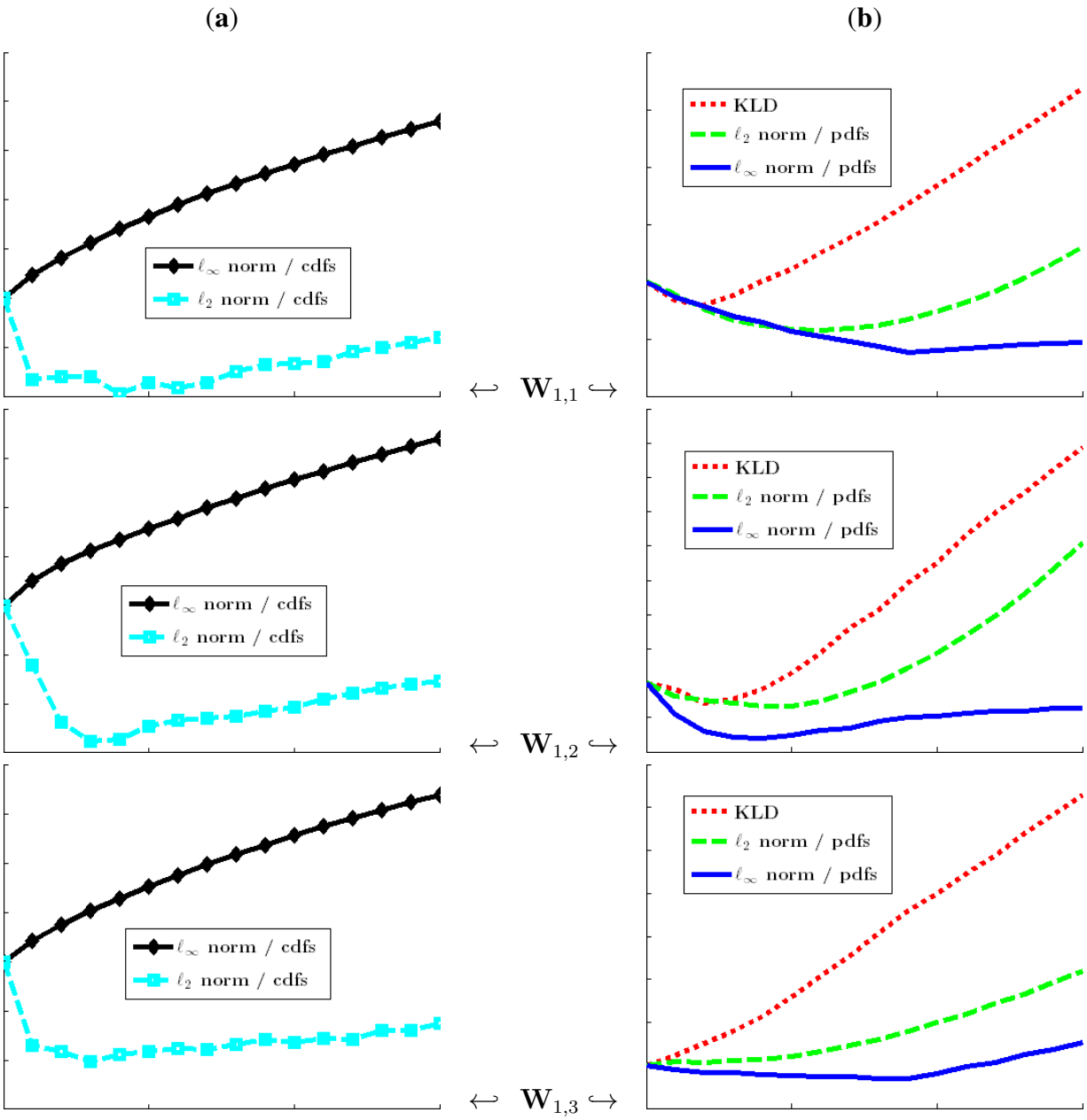

As can be seen in Figures 1 and 2, the uniform norm on the cdfs (Kolmogorov strategy) is the sole strategy that guarantees a non-decreasing relative stochasticity value (RSV; see Table 1) when the size K

of the pattern increases. Cumulative measures (ℓ_2, KLD), as well as pdf-based specifications, are not very relevant for stochasticity assessment, because of non-increasing deviations from the initial stochasticity degree: the local information is blurred through the averaging effect induced by cumulative measures or through neighborhood consideration when computing pdfs. Moreover, the same conclusion as above holds true when the experiments are performed on synthetic random numbers and without the use of wavelet transform.

From now on, we assume that the stochasticity parameter is of the Kolmogorov type: a uniform norm that applies for comparison of the empirical cdf with the distribution model. Section 3.1 addresses the choice of different bounds on this parameter for generating a semantic stochasticity template. This makes it possible to classify textures by mapping their sequences of stochasticity values on the stochasticity templates under consideration.

3. Classification From Wavelet Packet-Based Stochasticity Templates

3.1. Kolmogorov Stochasticity Measure versus *Error-Bounds from Image Estimation*

As shown in Section 2.2, the Kolmogorov parameter is relevant for detecting deterministic patterns in stochastic datasets and *vice versa*. For the main purpose of this paper, it is convenient to specify stochasticity bounds that make it possible to classify textures depending on their stochasticity degrees.

In the following, we derive different semantic classes consisting of stochasticity categories by fixing bounds on $\sup|F_{x,N}(t) - F(t)|$. This is performed by dealing with $\sup|F_{x,N}(t) - F(t)| < \eta_i$ as a problem of the estimation of an unknown function from observed samples and by fixing η_i, so as to guarantee a peak signal-to-noise ratio (PSNR) greater than Ω_idBs, where $(\Omega_i)_i$ are bounds taken from standards on PSNR quality from image denoising and compression problems.

The PSNR (peak signal-to-noise ratio, in decibel units, dB) is given by:

$$\text{PSNR} = 10\log_{10}\left(d^2/\text{MSE}\right) \tag{3}$$

where d is the dynamic of the image (the range of the pixel values $d = 255$ for eight-bit coded images) and MSE denotes the mean squared error.

Proposition 1 *Consider the problem of fitting $F_{x,N}(t_i)$ by $F(t_i)$ for $i = 1, 2, \ldots, N$. Then, in order to have a PSNR greater than ΩdBs, it suffices that*

$$\eta^2 \leqslant d \times 10^{-\Omega/10} \tag{4}$$

The dynamic of $F_{x,N}$ is one. Now, we set $\Omega_0 = 30$ dBs, $\Omega_1 = 35$ dBs and $\Omega_2 = 40$ dBs (a minimum of 30 dBs is required for an image denoising or compression algorithm to be relevant). These values are associated with the constants:

$$\eta_i = \sqrt{10^{-\Omega_i/10}}, \quad i = 0, 1, 2 \tag{5}$$

hereafter referred to as the lower bounds for high, good and fair quality set indicators. We will then use four stochasticity classes below:

Definition 1 (Semantic stochasticity classes) *A sample set x is said to be strongly stochastic (respectively stochastic, quasi-stochastic, non-stochastic) with respect to a continuous cdf, F, if $\kappa(x, F) \in [0, \eta_2]$ (respectively $\kappa(x, F) \in [\eta_2, \eta_1]$, $\kappa(x, F) \in [\eta_1, \eta_0]$, $\kappa(x, F) \in [\eta_0, +\infty]$).*

3.2. Texture Classification by Using Stochasticity Templates Upon Wavelet Packet Bases

Wavelet packet bases constitute a general framework for studying dictionaries of functional bases. Indeed, they offer a large family of functional bases with several properties, depending on whether we decide to split a given sub-band or not [23–26], among others. *Best basis* algorithms for the representation of signals involve seeking for functional atoms satisfying a given benchmark. In the wavelet framework, this benchmark is usually expressed in terms of the *energy* of the coefficients, the *sparsity*, or a number above a threshold, and entropy measurements [23,27,28]. Recent works on *best basis* algorithms concern compressive sensing and are related to the sparsity benchmark for piecewise regular images [29].

Hereafter, the best basis is computed upon the wavelet packet transform and under the stochasticity criterion: starting from the root node, $\mathbf{W}_{0,0}$, this consists of splitting every wavelet packet node $\mathbf{W}_{j,n}$ recursively, unless the stochasticity of a node has reached the fixed stochasticity bound. Indeed, the statistical properties of the wavelet packet coefficients (in particular, the higher order cumulant decay, see [18,20], among others) ensure that the Kolmogorov parameter decrease for a large class of stationary and non-stationary random processes. The corresponding algorithm is hereafter called BSB-WP (Best Stochastic Basis upon Wavelet Packets).

Table 2. VisTeX "Fabric" texture classification from Best Stochastic Basis upon Wavelet Packets (BSB-WP) stochasticity measurements. The "Fabric" textures are given in Figure 3. In this table, "Det" designates wavelet packet details and "Approx" designates wavelet approximations.

	Quasi-stochastic		**Stochastic**		**Strongly-stochastic**	
	Det.	Approx.	Det.	Approx.	Det.	Approx.
Fabric.18	√	√	√	√	√	–
Fabric.07	√	√	√	√	–	–
Fabric.17	√	√	√	–	–	–
Fabric.04	√	√	√	–	–	–
Fabric.09	√	√	√	–	–	–
Fabric.11	√	–	√	–	–	–
Fabric.15	√	–	√	–	–	–
Fabric.00	–	–	–	–	–	–
Fabric.14	–	–	–	–	–	–

We run the BSB-WP algorithm in order to classify the "Fabric" textures of the VisTeX database (see Figure 3). Stochasticity is measured with respect to cdfs pertaining to the exponential class

and the four semantic classes given in Definition 1 (non-stochastic, quasi-stochastic, stochastic and strongly-stochastic semantic classes). We used a maximum depth, J^*, fixed to four for the wavelet packet decomposition and the Daubechies wavelet of order seven. Table 2 summarizes the results obtained.

Figure 3. Texture "Fabrics" from the VisTeX database.

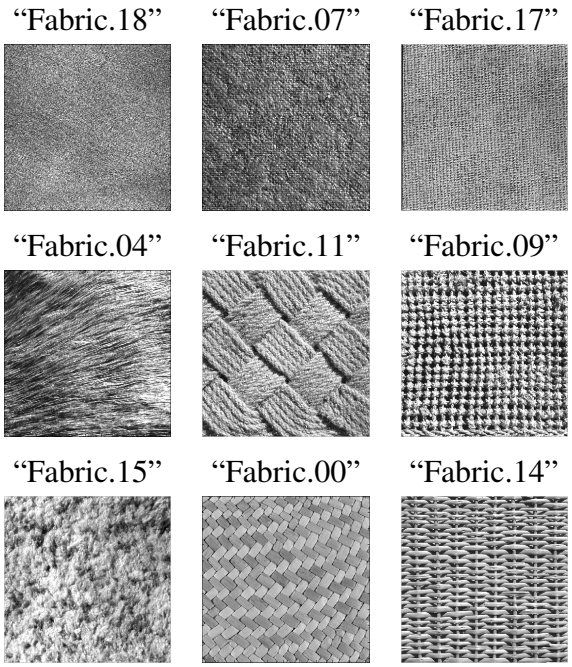

One can note that these results are consistent with the visual perception of randomness appearance. Furthermore, we derive from these results that textures "Fabric.18" and "Fabric.07" can be well characterized by using probabilistic distribution modeling applied on the nodes involved in their best bases. In contrast, probabilistic distribution modeling is not relevant for describing non-stochastic textures, such as "Fabric.00" and "Fabric.14", because their wavelet packet coefficient distribution deviates significantly from the continuous cdfs used. Note that the latter textures are regular, and thus, the appropriate criterion for their characterization needs to be based on regularity: regular images are sparse in the wavelet packet domain, and the sparsity criterion is thus expected to be more relevant.

The following provides some examples for illustrating BSB-WP texture characterization.

Example 1 *Texture "Fabric.07" is intrinsically quasi-stochastic:* $\kappa_{\textit{Fabric.07}} < \eta_0$. *BSB-WP provides a basis (see the basis composed of framed sub-bands in Figure 4) where all sub-bands involved in the representation are stochastic:* $\kappa_{c_{1,n}[\textit{Fabric.07}]} < \eta_1$ *for every* $n = 0, 1, 2, 3$. *The BSB-WP basis with a higher stochasticity property* ($\kappa < \eta_2$) *has not been found up to decomposition level* J^*.

Example 2 *Texture "Fabric.09" is not intrinsically stochastic:* $\kappa_{\textit{Fabric.09}} > \eta_0$. *BSB-WP provides a basis, where the texture can represented as a deterministic (smooth) approximation and stochastic details,* $\kappa_{c_{j,n}[\textit{Fabric.09}]} < \eta_1$, *for every nodes,* (j, n), *involved in the tree of Figure 5, with* $n \neq 0$.

Example 3 *Texture "Fabric.14" is not stochastic.* κ*-measurements are out of the stochasticity bounds for the input texture, as well as for many of its wavelet packet sub-bands up to decomposition level* J^*. *In addition, this texture presents a "singular" path in the sense given in* [18]. *Indeed, depending on the*

input process, some paths are such that no cdf regularization can be expected. In this case, stochasticity measures can increase as the decomposition level increases. This occurs for the path with sub-bands marked in oval frames in Figure 6.

Table 2 and Figure 3 highlight that stochasticity measurements in the wavelet domain are sensitive to the roughness/coarseness/coherence of textures and reflect the "randomness-appearance" of textures.

Figure 4. $100\times\kappa$ for texture "Fabric.07" from the VisTeX database. The BSB-WP is composed of framed sub-bands.

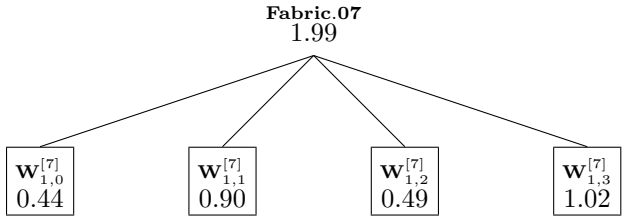

Figure 5. $100\times\kappa$ for texture "Fabric.09" from the VisTeX database. The BSB-WP is composed of framed sub-bands. The texture is represented as the sum of a smooth approximation and stochastic details.

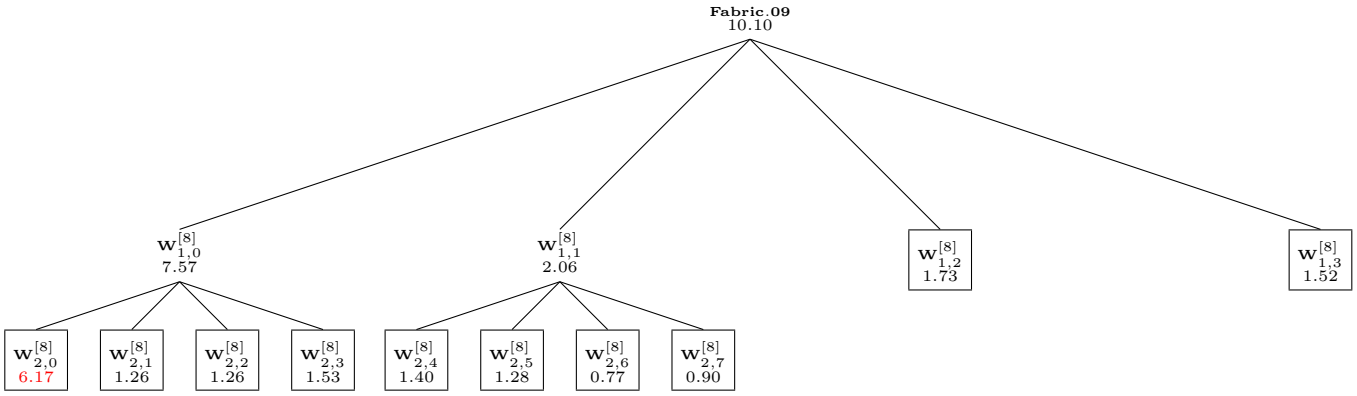

Figure 6. $100\times\kappa$ for texture "Fabric.14" from the VisTeX database at decomposition level 2. Many sub-bands remain non-stochastic. In addition, the stochasticity parameter, κ, does not systematically decrease as the decomposition level increases in some detail paths (see the path with the oval boxes).

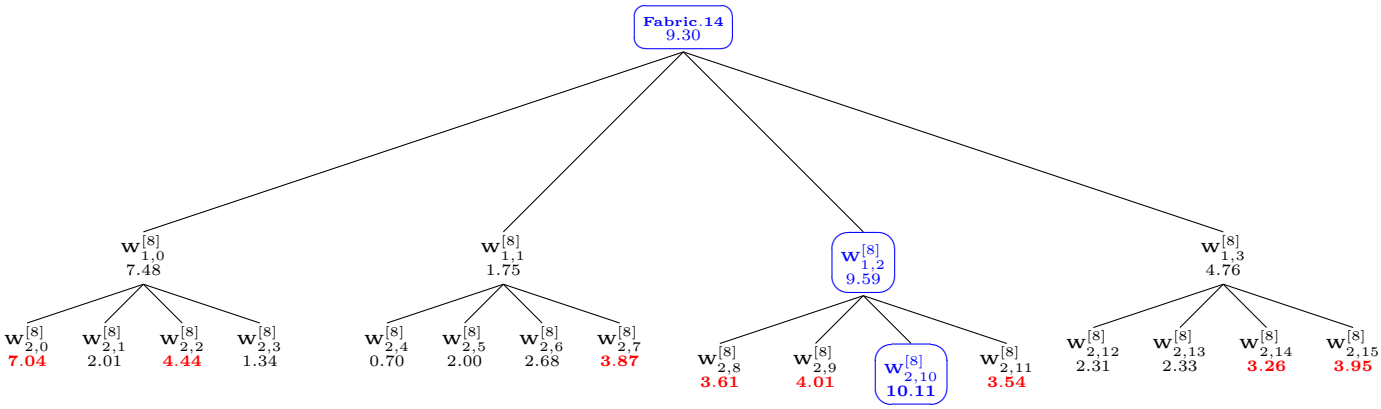

Table 3. Retrieval results per texture classes for 40 classes issued from the VisTeX database. Experimental results are performed without (blind approach) and with stochastic structuring, respectively. Stochastic texture classes are given in red, whereas non-stochastic classes are colored in blue, when considering stochastic structuring.

Blind approach				Stochastic structuring			
Texture	GG	WBL	PRT	Texture	GG	WBL	PRT
Bark.00	69.53	67.58	76.95	Bark.00	69.92	68.36	78.13
Bark.06	71.09	70.70	62.89	Bark.06	85.55	85.94	64.06
Bark.08	68.75	67.19	56.64	Bark.08	69.53	68.36	56.64
Bark.09	43.36	42.97	70.70	Bark.09	48.05	47.27	73.05
Bric.01	98.83	98.83	75.39	Bric.01	98.83	98.83	76.56
Bric.04	84.38	82.81	87.50	Bric.04	84.77	83.20	88.28
Bric.05	91.80	89.45	81.64	Bric.05	92.97	89.84	83.98
Buil.09	76.56	97.66	87.89	Buil.09	76.56	97.66	88.28
Fabr.00	87.89	86.72	78.13	Fabr.00	94.92	91.80	78.13
Fabr.04	86.72	86.72	81.64	Fabr.04	89.84	87.89	84.38
Fabr.07	98.05	98.05	75.39	Fabr.07	98.05	98.05	75.39
Fabr.09	100	100	80.47	Fabr.09	100	100	80.47
Fabr.11	92.58	92.58	57.81	Fabr.11	92.58	92.58	57.81
Fabr.14	100	100	89.45	Fabr.14	100	100	89.84
Fabr.15	92.58	92.19	57.03	Fabr.15	92.97	92.97	57.03
Fabr.17	92.58	96.09	85.16	Fabr.17	92.58	96.09	85.16
Fabr.18	94.92	91.80	47.27	Fabr.18	94.92	91.80	47.27
Flow.05	66.80	65.63	80.47	Flow.05	68.36	66.41	80.86
Food.00	96.48	96.48	84.77	Food.00	100	100	87.50
Food.05	78.91	78.91	72.27	Food.05	81.64	81.64	72.27
Food.08	99.61	100	86.33	Food.08	99.61	100	86.33
Gras.01	98.83	98.83	52.73	Gras.01	98.83	98.83	53.13
Leav.08	74.22	73.44	80.86	Leav.08	82.03	83.20	80.86
Leav.10	61.72	60.94	76.17	Leav.10	64.84	63.67	77.34
Leav.11	67.58	66.80	87.11	Leav.11	73.05	72.66	87.50
Leav.12	78.13	78.52	53.91	Leav.12	98.05	97.27	53.91
Leav.16	72.27	71.48	87.11	Leav.16	72.27	71.48	87.11
Meta.00	83.20	82.42	59.38	Meta.00	83.20	82.42	59.38
Meta.02	100	100	86.33	Meta.02	100	100	86.33
Misc.02	96.09	95.70	56.64	Misc.02	96.09	95.70	56.64
Sand.00	96.48	97.66	51.56	Sand.00	96.48	97.66	51.56
Ston.01	73.83	74.61	78.13	Ston.01	73.83	74.61	78.13
Ston.04	93.75	92.97	49.22	Ston.04	93.75	92.97	49.22
Terr.10	55.08	53.52	87.89	Terr.10	63.28	62.50	88.28
Tile.01	62.11	61.72	91.41	Tile.01	62.11	61.72	91.41
Tile.04	99.61	99.61	94.14	Tile.04	99.61	99.61	94.14
Tile.07	98.05	97.66	83.98	Tile.07	99.22	98.83	83.98
Wate.05	100	100	56.25	Wate.05	100	100	56.25
Wood.01	57.42	56.64	75.39	Wood.01	61.33	61.33	75.78
Wood.02	100	100	66.41	Wood.02	100	100	67.58

4. Content-Based Image Retrieval with Stochastic Structuring

In what follows, $\mathcal{T}$ denotes a texture database assumed to be heterogeneous in the sense that it contains both stochastic and regular textures. We consider the problem of structuring the elements of $\mathcal{T}$ by using the stochasticity degree. The structuring proposed is a splitting of database $\mathcal{T}$ into two metaclasses: stochastic *versus* regular textures. This structuring will be used as a pre-classification for level 1 content-based image retrieval (CBIR), based on parametric modeling of the statistical distributions of the wavelet coefficients. In this standard 1 CBIR [30], the query is completely specified through the statistical distributions of texture pixel values.

4.1. Stochastic Structuring

The structuring is performed with respect to the stochasticity measurements in the wavelet domain. The wavelet transform used is the stationary wavelet transform (SWT). Indeed, the SWT is appreciated for its shift-invariance property and is known to be relevant for the level 1 CBIR under consideration [31].

We consider the Edgeworth expansions of order four for modeling the SWT approximation sub-bands and the generalized Gaussian, Pareto and Weibull distributions for modeling the detail of the SWT coefficients. Model validation regarding the above issues can be found in [31]. The symmetric Kullback-Leibler divergence is used as a similarity measure between the statistical distributions given above.

Experimental tests concern 40 texture classes of the VisTeX database. The database structuring for these classes is given, in terms of stochastic *versus* regular textures, in Table 3: this structuring yields a stochastic metaclass composed of 22 texture classes and a regular metaclass composed of 18 texture classes.

4.2. Content-Based Image Retrieval on Structured Databases

This section provides CBIR experimental results on structured databases, in comparison with the results obtained without stochastic structuring. The experimental setup is the one used in [31]: any texture class (among the 40 texture classes considered) is composed of 16 images obtained by splitting every large texture image into 16 non-overlapping subimages. Thus, we have a test database, $\mathcal{T}$, composed of 640 images, among which 352 images forming a database structure, $\mathcal{T}_1$, are issued from a stochastic class; whereas the 288 remaining textures constitute a database structure, $\mathcal{T}_2$, associated with regular texture classes, with $\mathcal{T} = \mathcal{T}_1 \cup \mathcal{T}_2$.

We then run CBIR from parametric modeling and similarity measurements, as described in [31], with the symlet wavelet of order eight. Experimental tests are performed independently on the tree database structures, $\mathcal{T}_1, \mathcal{T}_2 and \mathcal{T}$. For a given structure, performance measurements concern the retrieval rates, when a query is any subimage of the structure under consideration. Retrieval rates per class are given in Table 3 concerning $\mathcal{T}_1$ and $\mathcal{T}_2$. Average retrieval rates per structures $\mathcal{T}_1, \mathcal{T}_2 and \mathcal{T}$ are given in Table 4 for comparison purposes.

Table 4. The average values of texture-specific retrieval for the whole database, $\mathcal{T}$, the database composed of *stochastic textures*, $\mathcal{T}_1$, and the database composed of *regular textures*, $\mathcal{T}_2$, with $\mathcal{T}_1 \cup \mathcal{T}_2 = \mathcal{T}$. Experimental results performed without stochastic structuring (blind approach) are given for comparison purposes.

Stochastic textures ($\mathcal{T}_1$)					
Blind approach			Stochastic structuring		
GG	WBL	PRT	GG	WBL	PRT
88.12	**87.82**	**66.05**	**90.45**	**90.02**	**66.67**
Regular textures ($\mathcal{T}_2$)					
Blind approach			Stochastic structuring		
GG	WBL	PRT	GG	WBL	PRT
78.95	**79.60**	**83.18**	**81.10**	**81.81**	**83.51**
Whole texture database ($\mathcal{T}$)					
Blind approach			Stochastic structuring		
GG	WBL	PRT	GG	WBL	PRT
83.99	**84.12**	**73.76**	**86.24**	**86.33**	**74.25**

From Table 4, it follows that the retrieval is more concise when the search focuses either on $\mathcal{T}_1$ or on $\mathcal{T}_2$ than on the whole structure, $\mathcal{T}$. Since $\mathcal{T}_1$ and $\mathcal{T}_2$ have low cardinality, the structuring also eases the search. In addition, from Table 4 and when comparing the role played by the distribution type on the metaclass, it follows that the more relevant family is:

- the GG family for modeling the stochastic textures,
- the PRT family for modeling the regular textures,
- the WBL family for modeling the whole database containing both regular and stochastic textures.

The above remarks confirm the suitability of separating a heterogeneous database into structures with approximately the same stochasticity degrees.

5. Content-Based Stochasticity Retrieval

This section addresses stochasticity considerations for CBIR feature selection in texture databases. This CBIR takes into account the inference made in Section 3 for deriving different stochasticity templates. It is worth noting that the stochasticity degree can be seen as an index aggregating many low-level texture features (statistical distributions) in order to derive a high-level feature: the randomness-like appearance of a dataset. In this respect, we are concerned with the level 2 CBIR [30]. The motivation in using a stochasticity criterion for level 2 CBIR is the following.

Consider a geometrically regular image (a human face, textures "Fabric.00" and "Fabric.14" given in Figure 3, *etc*). For such an image, the form (through primitives) and the regularity are known to be

relevant features for content description [10,32]. Consider now a stochastic texture (see, for instance, "Fabric.18" and "Fabric.07"). Such a texture is not regular and has no structured components that can be taken as feature descriptors. In contrast, the randomness appearance measured by the stochasticity parameter is appealing in differencing textures "Fabric.18" and "Fabric.07": stochasticity is an index that addresses the intrinsic coherence (non-coherence being close to stochasticity) of the texture.

The following provides two CBIR strategies based on stochasticity measurements and referred to as content-based stochasticity retrieval (CBSR): (1) CBSR by learning the stochasticity tree structure characterizing the BSB-WP of some texture training samples; and (2) CBSR by generating the stochasticity template from a set of training texture samples, given a fixed wavelet packet basis.

5.1. Content-Based Stochasticity Retrieval by Learning the Stochasticity Tree Structure

In this section, we consider a set of M texture classes indexed by integer $m, 1 \leqslant m \leqslant M$. For a given class, m, we assume that samples $(m_k)_{k=1,2,\ldots K_m}$ are available (learning database). Let $\mathtt{B}_{\text{Best}}[m_k]$ denote the BSB-WP associated with sample m_k at the fixed stochasticity degree, η.

Consider the smallest (infimum) and the largest (supremum) wavelet packet tree structures of the BSB-WP trees associated with samples $(m_k)_k$ of texture class m. These trees define some wavelet packet bases denoted respectively by:

$$\mathtt{B}^{\inf}[m] = \inf\left\{\mathtt{B}_{\text{Best}}[m_1], \mathtt{B}_{\text{Best}}[m_2], \ldots, \mathtt{B}_{\text{Best}}[m_{K_m}]\right\}$$

$$\mathtt{B}^{\sup}[m] = \sup\left\{\mathtt{B}_{\text{Best}}[m_1], \mathtt{B}_{\text{Best}}[m_2], \ldots, \mathtt{B}_{\text{Best}}[m_{K_m}]\right\}$$

In this respect, we will say that the tree structure describing the behavior of the best stochastic representations of the samples of texture m have lower bound $\mathtt{B}^{\inf}[m]$ and upper bound $\mathtt{B}^{\sup}[m]$.

The CBSR principle considered in this section is the following: an arbitrary sample belongs to stochasticity class m if its best basis at stochasticity degree η, denoted by $\mathtt{B}$, is such that $\mathtt{B}^{\inf}[m] \preceq \mathtt{B} \preceq \mathtt{B}^{\sup}[m]$.

Consider the set of "Fabric" textures from the VisTeX database (see Figure 3). From the classification obtained in Table 2, we focuses on "Fabric.0007" and "Fabric.0018", which are closer on the basis of their stochasticity degrees. We set the stochasticity degree to η_2. We then consider the following experimental setup: each image is split into 16 non-overlapping subimages; $K = 8$ images among them (the eight upper-half subimages) are used as the training set. The remaining 16 subimages, eight subimages of 'Fabric.0007" and eight subimages of "Fabric.0018", the lower-half subimages, are put together to form the test database.

We run the following CBSR strategy:

- *Learn* the stochasticity tree structure for any of the "Fabric" textures by computing $\mathtt{B}^{\inf}$ and $\mathtt{B}^{\sup}$ from its eight, samples available from the learning database.
- *Retrieve*, from the test database, the samples that belong to the semantic class of any of the "Fabric" textures, that are the samples having stochasticity bases bounded by the infimum and supremum bases associated with the class.
- *Sort* the samples thus obtained, and compute texture-specific retrieval.

From the experiments carried out, we have that:

- The learned basis structure corresponding to "Fabric.0007" is any basis, B, such that:

$$\bigcup_{n=0,1,2,3} \mathbf{W}_{1,n} \preceq \mathtt{B} \preceq \mathbf{W}_{2,0} \cup \left(\bigcup_{n=4,5,\ldots,4^3-1} \mathbf{W}_{3,n} \right) \tag{6}$$

- The learned basis structure for "Fabric.0018" is any basis B, such that:

$$\mathbf{W}_{2,0} \cup \left(\bigcup_{j=1,2} \bigcup_{n=1,2,3} \mathbf{W}_{j,n} \right) \preceq \mathtt{B} \preceq \mathbf{W}_{3,0} \cup \left(\bigcup_{j=1,2,3} \bigcup_{n=1,2,3} \mathbf{W}_{j,n} \right) \tag{7}$$

The retrieval rates obtained from the test database are such that:

- Query "Fabric.0007", associated with the lowest randomness degree among the two classes, reduces the search database from 16 to eight, including seven good retrievals/eight.
- Query "Fabric.0018", associated with the highest randomness degree among the two classes, reduces the search database from 16 to seven, including seven good retrievals/eight.

From these experiments, stochasticity, as a feature measuring the intrinsic coherence of a texture, can be used to generate a stochasticity tree structure representing the BSB-WPs, a texture observed through some training samples.

5.2. Content-Based Stochasticity Retrieval by Learning the Stochasticity Bounds

Depending on constraints, such as computational load or dealing with a large number of semantic classes, it may sometimes be desirable to fix the decomposition basis. In this section, we consider a fixed wavelet packet basis $\mathtt{B} = \bigcup_{p=1,2,\ldots,L} \mathbf{W}_{J_p,n_p}$ and propose high-level CBSR by computing, from training samples, the subspace within which the stochasticity parameters are expected to lie.

Assume the availability of K samples (subimages) for every texture class, m, considered, with $1 \leqslant m \leqslant M$ (the training set for this texture). Let us denote by $\kappa_{m_\ell}(J_p, n_p)$ the value of the stochasticity parameter (see Equation (1)) associated with the sub-band, $\mathbf{W}_{J_p,n_p}$, coefficients of subimage m_ℓ. The sequence $(\kappa_{m_\ell}(J_p, n_p))_{\ell=1,2,\ldots,K}$ represents the behavior of the stochasticity parameters of the projection of texture m samples on sub-band $\mathbf{W}_{J_p,n_p}$. Let us denote $\kappa^m_{\min}(J_p, n_p) = \min\{\kappa_{m_\ell}(J_p, n_p), \ell = 1, 2, \ldots, K\}$ and $\kappa^m_{\max}(J_p, n_p) = \max\{\kappa_{m_\ell}(J_p, n_p), \ell = 1, 2, \ldots, K\}$. Define the stochasticity hypercube associated with the samples of texture m on basis B by:

$$\mathcal{H}^m_L = \prod_{p=1}^{L} \left[\kappa^{\min}_m(J_p, n_p), \kappa^{\max}_m(J_p, n_p)\right] \tag{8}$$

The CBSR principle considered in this section is the following: it is decided that a query sample admitting stochasticity parameters, $\kappa(J_1, n_1), \kappa(J_2, n_2) and \ldots, \kappa(J_L, n_L)$, on basis B belongs to class m if the vector $(\kappa(J_1, n_1), \kappa(J_2, n_2), \ldots, \kappa(J_L, n_L)) \in \mathcal{H}^m_L$.

In this respect, a texture can be characterized by the hypercube defined from the lower and upper bounds of the stochasticity parameters of its sample coefficients on the basis, B. This hypercube defines the semantic class of the texture.

Assume that a new sample of the texture is available. Then, we can re-evaluate the stochasticity bounds when some of the additional stochasticity parameters of this sample are out of the texture stochasticity hypercube. In addition, depending on the distribution of the stochasticity parameters, the user can discard those behaving as outliers in order to tighten the stochasticity hypercube and avoid overlapping with stochasticity hypercubes associated with other semantic classes. This re-evaluation is known to be useful in integrated CBIR systems [33].

The following provides CBSR experimental results obtained for $M = 40$ textures from the VisTeX database. The experimental setup used is described below:

- First, we construct the learning database by using the top-half of the images: each top-half image is split into $K = 8$ non-overlapping subimages (128×128 pixels per subimage). These K subimages are used to compute the stochasticity hypercube $\mathcal{H}_L^m$ for $m = 1, 2, \ldots, 40$.
- Then, we constitute the test database by using the down-half of the images: each down-half image is split into eight non-overlapping subimages. Thus, the test database is composed of $8 \times M$ subimages.
- In order to increase the number of experiments, we have also permutated the roles played by the learning and the test database (the top-half becomes the down-half and *vice-versa*).

We run this procedure when the decomposition is performed by using a wavelet basis with $J^* = 2$. The stochasticity is measured with respect to dictionary $\mathcal{D}$ (Table 5a) and with respect to a single distribution family: the GG distributions (Table 5b). Specifically, in these tables, we have that two stochasticity coordinates out of $\mathcal{H}_L^m$ are tolerated, that is, two stochasticity parameters that are out-of-bounds are tolerated among a set of $3 * J^* + 1 = 7$ stochasticity parameters $\kappa(J_1, n_1), \kappa(J_2, n_2), \ldots, \kappa(J_L, n_L)$ with $L = 7$. In Tables 5, TPR denotes the true positive rate defined as the ratio (the fraction of relevant queries per class):

$$\text{TPR}[m] = \frac{\text{Number of admissible subimages thatare issued from texture } m}{\text{Total number of relevant subimages}}$$

and FAR denotes the false alarm rate per class:

$$\text{FAR}[m] = \frac{\text{Number of admissible subimages thatare not issued from texture } m}{\text{Total number of subimages that are not issued from texture } m}$$

Table 5. (**a**) True positive rate (TPR) and false alarm rate (FAR) for content-based stochasticity retrieval (CBSR) by learning the stochasticity bounds. Dictionary $\mathcal{D}$ is used for stochasticity measurements; (**b**) True positive rate (TPR) and false alarm rate (FAR) for CBSR by learning the stochasticity bounds. The GG family is used for stochasticity measurements.

Texture	TPR	FAR
Bark.00	62.50	08.97
Bark.06	37.50	07.69
Bark.08	62.50	00.80
Bark.09	75.00	10.58
Bric.01	31.25	01.44
Bric.04	37.50	02.56
Bric.05	50.00	06.89
Buil.09	37.50	00.96
Fabr.00	43.75	01.92
Fabr.04	50.00	07.05
Fabr.07	62.50	01.12
Fabr.09	37.50	00.48
Fabr.11	56.25	01.44
Fabr.14	50.00	0
Fabr.15	68.75	00.80
Fabr.17	56.25	01.12
Fabr.18	68.75	00.48
Flow.05	31.25	07.21
Food.00	62.50	01.92
Food.05	31.25	03.21
Food.08	56.25	0
Grass.01	37.50	04.81
Leav.08	68.75	12.66
Leav.10	43.75	09.13
Leav.11	56.25	04.65
Leav.12	43.75	04.65
Leav.16	62.50	01.92
Meta.00	50.00	01.92
Meta.02	68.75	00.32
Misc.02	62.50	00.64
Sand.00	31.25	02.24
Ston.01	56.25	08.01
Ston.04	62.50	01.92
Terr.10	50.00	08.01
Tile.01	31.25	02.40
Tile.04	37.50	00.96
Tile.07	25.00	0
Wate.05	62.50	02.40
Wood.01	56.25	12.18
Wood.02	56.25	09.29

(**a**)

Texture	TPR	FAR
Bark.00	100	18.27
Bark.06	75.00	13.78
Bark.08	68.75	03.37
Bark.09	75.00	20.83
Bric.01	62.50	03.85
Bric.04	68.75	04.01
Bric.05	75.00	08.97
Buil.09	56.25	02.56
Fabr.00	62.50	02.88
Fabr.04	50.00	13.62
Fabr.07	81.25	01.44
Fabr.09	75.00	00.64
Fabr.11	81.25	02.40
Fabr.14	87.50	00.16
Fabr.15	87.50	02.08
Fabr.17	87.50	03.05
Fabr.18	81.25	01.12
Flow.05	56.25	11.06
Food.00	93.75	02.56
Food.05	50.00	04.17
Food.08	75.00	00.48
Grass.01	50.00	07.85
Leav.08	75.00	16.03
Leav.10	56.25	14.58
Leav.11	62.50	06.89
Leav.12	43.75	04.81
Leav.16	75.00	02.56
Meta.00	68.75	02.72
Meta.02	87.50	00.64
Misc.02	68.75	00.96
Sand.00	62.50	03.37
Ston.01	62.50	13.94
Ston.04	68.75	03.53
Terr.10	68.75	16.35
Tile.01	37.50	04.17
Tile.04	68.75	02.08
Tile.07	31.25	0
Wate.05	81.25	07.69
Wood.01	93.75	24.20
Wood.02	75.00	15.22

(**b**)

As can be seen in these tables, stochasticity-based retrieval is relevant for most textures given in this database. Low TPRs occur when texture is very regular (Example: "Tile.0001", "Tile.0007"); see Figure 7. High FARs occur when textures have non-homogeneous subimages (Example: "Wood.0001"): the bounds define a large interval, which is expected to contain stochasticity values related to many other textures; see Figure 7.

Figure 7. Textures "Tile.0001", "Tile.0007", "Wood.0001" from the VisTeX album.

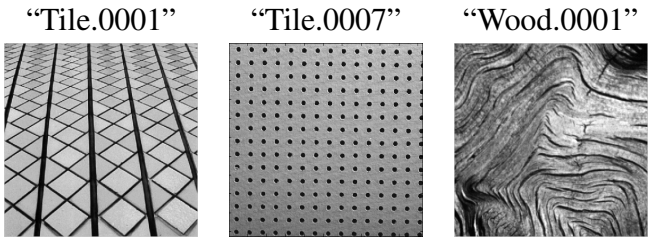

Experiments on the Brodatz album yield approximately the same results. The global TPR is 69% for the Brodatz album (respectively 70% for the VisTeX album) and the global FAR is 10% for the Brodatz album (respectively 7% for the VisTeX album), when GG modeling is used for stochasticity measurements. Tables concerning the Brodatz album are omitted, because the tests are concerned with 111 textures.

6. Conclusions

The paper has addressed texture image description and understanding through stochasticity or randomness appearance. The framework used for measuring stochasticity is that of the wavelet bases, because of their suitable statistical properties. The Kolmogorov stochasticity parameter is shown to be relevant for pointing out deterministic smooth patterns from wavelet coefficients of textures. The relevance of the stochasticity consideration is proven to be efficient for classification, database structuring and content-based image retrieval involving textured images.

Open issues related to this work may concern the analysis and the interpretation of the sequence of wavelet sub-band stochasticity parameters. In this work, we have considered the whole stochasticity hypercube obtained from the minimum and the maximum values of the stochasticity parameters of texture training samples. However, more investigations need to be performed in order to derive, among these sequences of parameters, some clusters or the manifold that describes the observed stochasticity sequences well.

Conflicts of Interest

The authors declare no conflict of interest.

References

1. Korostelev, A.P.; Tsybakov, A.B. *Minimax Theory of Image Reconstruction*; Springer: New York, NY, USA, 1993.

2. Tamura, H.; Mori, S.; Yamawaki, T. Textural features corresponding to visual perception. *IEEE Trans. Syst. Man Cybern.* **1978**, *8*, 460–473.
3. Vasselle, B.; Giraudon, G. A multiscale regularity measure as a geometric criterion for image segmentation. *Mach. Vision Appl.* **1994**, *7*, 229–236.
4. Manjunath, B.S.; Ohm, J.; Vasudevan, V.V.; Yamada, A. Color and texture descriptors. *IEEE Trans. Circuits Syst. Video Technol.* **1998**, *11*, 703–715.
5. Chetverikov, D. Pattern regularity as a visual key. *Image Vision Comput.* **2000**, *18*, 975–985.
6. Fujii, K.; Sugi, S.; Ando, Y. Textural properties corresponding to visual perception based on the correlation mechanism in the visual system. *Psychol. Res.* **2003**, *67*, 197–208.
7. Trujillo, L.; Olague, G.; Legrand, P.; Lutton, E. Regularity based descriptor computed from local image oscillations. *Opt. Express* **2007**, *15*, 6140–6145.
8. Daugmann, J.G. Uncertainty relation for resolution in space, spatial frequency, and orientation optimized by two-dimensional visual cortical filters. *J. Opt. Soc. Am. A* **1985**, *2*, 1160–1169.
9. Liu, F.; Picard, R.W. Periodicity, directionality, and randomness: Wold features for image modeling and retrieval. *IEEE Trans. Pattern Anal. Mach. Intell.* **1996**, *18*, 722–733.
10. Wang, J.Z.; Li, J.; Wiederhold, G. SIMPLIcity: Semantics-sensitive integrated matching for picture libraries. *IEEE Trans. Pattern Anal. Mach. Intell.* **2001**, *23*, 947–963.
11. Stitou, Y.; Turcu, F.; Berthoumieu, Y.; Najim, M. Three-dimensional textured image blocks model based on wold decomposition. *IEEE Trans. Signal Process.* **2007**, *55*, 3247–3261.
12. Unser, M. Texture classification and segmentation using wavelet frames. *IEEE Trans. Image Process.* **1995**, *4*, 1549–1560.
13. Mondal, D.; Percival, D. Wavelet variance analysis for random fields on a regular lattice. *IEEE Trans. Image Process.* **2012**, *21*, 537–549.
14. Geilhufe, M.; Percival, D.; Stern, H. Two-dimensional wavelet variance estimation with application to sea ice **SAR** images. *Comput. Geosci.* **2013**, *54*, 351–360.
15. Kolmogorov, A.N. Sulla determinazione empirica di una legge di distribuzione. *Giornale dell'Istituto Italiano degli Attuari*, **1933**, *4*, 83–91, (in Italian).
16. Arnold, V. Orbits' statistics in chaotic dynamical systems. *Nonlinearity* **2008**, *21*, T109–T112.
17. Gurzadyan, V.G.; Kocharyan, A.A. Kolmogorov stochasticity parameter measuring the randomness in the cosmic microwave background. *Astron. Astrophys.* **2008**, *492*, L33–L34.
18. Atto, A.M.; Berthoumieu, Y. Wavelet packets of nonstationary random processes: Contributing factors for stationarity and decorrelation. *IEEE Trans. Inf. Theory* **2012**, *58*, 317–330.
19. Atto, A.M.; Pastor, D.; Mercier, G. Wavelet packets of fractional brownian motion: Asymptotic analysis and spectrum estimation. *IEEE Trans. Inf. Theory* **2010**, *56*, 4741–4753.
20. Atto, A.M.; Pastor, D. Central limit theorems for wavelet packet decompositions of stationary random processes. *IEEE Trans. Signal Process.* **2010**, *58*, 896–901.
21. Massey, J.F.J. The Kolmogorov-Smirnov test for goodness of fit. *J. Am. Stat. Assoc.* **1951**, *253*, 68–78.
22. Kenney, J.F.; Keeping, E.S. *Mathematics of Statistics, Part II*; Van Nostrand Company, Inc: Princeton, NJ, USA, 1951.

23. Wickerhauser, M.V. Inria Lectures on Wavelet Packet Algorithms. In *Problèmes Non-Linéaires Appliqués, Ondelettes et Paquets D'Ondes*; Lions, P.-L., Ed.; INRIA: Roquencourt, France, 1991; pp. 31–99.
24. Daubechies, I. *Ten Lectures on Wavelets*; SIAM: Philadelphie, PA, USA, 1992.
25. Coifman, R.R.; Wickerhauser, M.V. Entropy-based algorithms for best basis selection. *IEEE Trans. Inf. Theory* **1992**, *38*, 713–718.
26. Hess-Nielsen, N.; Wickerhauser, M.V. Wavelets and time-frequency analysis. *Proc. IEEE* **1996**, *84*, 523–540.
27. Laine, A.; Fan, J. Texture classification by wavelet packet signatures. *IEEE Trans. Pattern Anal. Mach. Intell.* **1993**, *15*, 1186–1191.
28. Chang, T.; Kuo, C.-C.J. Texture analysis and classification with tree-structured wavelet transform. *IEEE Trans. Image Process.* **1993**, *2*, 429–441.
29. Peyré, G. Best basis compressed sensing. *IEEE Trans. Signal Process.* **2010**, *58*, 2613–2622.
30. Eakins, J.; Graham, M. *Content-Based Image Retrieval*; Technical Report; University of Northumbria: Newcastle, UK, 1999.
31. Atto, A.M.; Berthoumieu, Y. How to Perform Texture Recognition from Stochastic Modeling in the Wavelet Domain. In Proceedings of IEEE International Conference on Acoustics, Speech, and Signal Processing (ICASSP), Prague, Czech Republic, 22–27 May 2011; pp. 4320–4323.
32. Liu, Y.; Zhang, D.; Lu, G.; Ma, W.-Y. A survey of content-based image retrieval with high-level semantics. *Pattern Recognit.* **2007**, *40*, 262–282, .
33. Smeulders, A.W.M.; Worring, M.; Gupta, A.; Jain, R. Content-based image retrieval at the end of the early years. *IEEE Trans. Pattern Anal. Mach. Intell.* **2000**, *22*, 1349–1380.